PROCEEDINGS OF SPIE

SPIEDigitalLibrary.org/conference-proceedings-of-spie

On the alignment and focusing of the Marshall Grazing Incidence X-ray Spectrometer (MaGIXS)

Patrick Champey, Amy Winebarger, Ken Kobayashi, Sabrina Savage, Jonathan Cirtain, et al.

Patrick Champey, Amy Winebarger, Ken Kobayashi, Sabrina Savage, Jonathan Cirtain, Peter Cheimets, Edward Hertz, Leon Golub, Brian Ramsey, Jeff McCracken, Vanessa Marquez, Ryan Allured, Ralf K. Heilmann, Mark Schattenburg, Alexander Bruccoleri, "On the alignment and focusing of the Marshall Grazing Incidence X-ray Spectrometer (MaGIXS)," Proc. SPIE 9905, Space Telescopes and Instrumentation 2016: Ultraviolet to Gamma Ray, 990573 (18 July 2016); doi: 10.1117/12.2232820

SPIE.

Event: SPIE Astronomical Telescopes + Instrumentation, 2016, Edinburgh, United Kingdom

On the Alignment and Focusing of the Marshall Grazing Incidence X-ray Spectrometer (MaGIXS)

Patrick Champey[*a,b], Amy Winebarger[b], Ken Kobayashi[b], Sabrina Savage[b], Jonathan Cirtain[b], Peter Cheimets[c], Edward Hertz[c], Leon Golub[c], Brian Ramsey[b], Jeff McCracken[b], Vanessa Marquez[c], Ryan Allured[c], Ralf K. Heilmann[d], Mark Schattenburg[d], and Alexander Bruccoleri[e]

[a]The University of Alabama in Huntsville, Huntsville, AL, United States
[b]NASA Marshall Space Flight Center, Huntsville, AL, United States
[c]Smithsonian Astrophysical Observatory, Cambridge, MA, United States
[d]Massachusetts Institute of Technology, Cambridge, MA, United States
[e]Izentis LLC, Cambridge, MA, United States

ABSTRACT

The Marshall Grazing Incidence X-ray Spectrometer (MaGIXS) is a NASA sounding rocket instrument that is designed to observe soft X-ray emissions from 24 - 6.0 Å (0.5 - 2.0 keV energies) in the solar atmosphere. For the first time, high-temperature, low-emission plasma will be observed directly with 5 arcsecond spatial resolution and 22 mÅ spectral resolution. The unique optical design consists of a Wolter - I telescope and a 3-optic grazing-incidence spectrometer. The spectrometer utilizes a finite conjugate mirror pair and a blazed planar, varied line spaced grating, which is directly printed on a silicon substrate using e-beam lithography. The grating design is being finalized and the grating will be fabricated by the Massachusetts Institute of Technology (MIT) and Izentis LLC. Marshall Space Flight Center (MSFC) is producing the nickel replicated telescope and spectrometer mirrors using the same facilities and techniques as those developed for the ART-XC and FOXSI mirrors. The Smithsonian Astrophysical Observatory (SAO) will mount and align the optical sub-assemblies based on previous experience with similar instruments, such as the Hinode X-Ray Telescope (XRT). The telescope and spectrometer assembly will be aligned in visible light through the implementation of a theodolite and reference mirrors, in addition to the centroid detector assembly (CDA) – a device designed to align the AXAF-I nested mirrors. Focusing of the telescope and spectrometer will be achieved using the X-ray source in the Stray Light Facility (SLF) at MSFC. We present results from an alignment sensitivity analysis performed on the on the system and we also discuss the method for aligning and focusing MaGIXS.

Keywords: X-ray, Alignment, Sounding Rocket

1. INTRODUCTION

High temperature plasma, 10^6 to 10^7 K range, in the solar corona produces strong emission in the soft X-ray spectrum. Knowledge of the heating mechanisms in this region of the solar atmosphere is limited, partly because detailed observations and measurements of the temperature distribution of the plasma are not readily available. MaGIXS is designed to probe the high-temperature coronal plasma and provide insight to the nature of coronal heating. At these higher temperatures, different heating mechanisms result in different differential emission measure (DEM) distribution. Key spectral lines that MaGIXS will observe are:

*patrick.r.champey@nasa.gov

Space Telescopes and Instrumentation 2016: Ultraviolet to Gamma Ray, edited by
Jan-Willem A. den Herder, Tadayuki Takahashi, Marshall Bautz, Proc. of SPIE Vol. 9905, 990573
 · doi: 10.1117/12.2232820

Spectral Line	Wavelength [Å]	Energy [keV]	Log Temp.
Mg XII	8.42	1.47	6.9
Mg XI	9.16	1.35	6.4
Ne X	12.13	1.02	6.6
Fe XX	12.85	0.96	7.0
Ne IX	13.45	0.92	6.2
Fe XIX	13.52	0.92	6.9
Fe XVIII	14.21	0.87	6.8
Fe XVII	15.01	0.83	6.6
O VIII	18.97	0.65	6.4
O VII	21.6	0.57	6.3

Table 1: Key spectral lines observed by MaGIXS

These spectral lines should be observed with resolution better than 22 mÅ. Additionally, fine structures along the slit must be resolved to 5 arcseconds, or better. An observational target suitable for these measurements is a medium-sized active region, on the order of 400 arcseconds across. The slit should be long enough to subtend the active region; MaGIXS slit length is 460 arcseconds (8 arcminutes). Below are the instrument specifications.

- Spectral band: 24 - 6 Å(0.5 - 2.0 keV)
- Spectral resolution: 22 mÅ(0.47 - 7.5 eV)
- Spectral plate scale: 11 mÅ/pixel (0.25 - 3.8 eV/pixel)
- Spatial Resolution: 5 arcseconds
- Spatial plate scale: 2.8 arcseconds/pixel
- Slit: 8 arcminutes
- Cadence: <5 seconds

MaGIXS is a full grazing incidence imaging spectrometer, composed of 4 optical elements and a CCD detector.[1,2] The instrument will observe soft X-ray spectrum from 24 - 6.0 Å(0.5 - 2.0 keV) with a spatially resolved component along the 8 arcmin long slit. The slit is placed at the focal plane of a single shell, nickel-replicated Wolter-I telescope. On the back side of the slit is a finite conjugate mirror pair, a grating and CCD detector. The optical layout is shown in Figure 1 and Figure 2 is the mechanical layout of the payload. The finite conjugate mirror pair are identical nickel-replicated paraboloidal mirror shells (SM1 and SM2, respectively). The Wolter-I telescope and paraboloidal mirror pair are being produced by Marshall Space Flight Center (MSFC) using the same electroform nickel-replication techniques developed for instruments such as ART-XC[3,4] and FOXSI.[5–7] Currently the mandrels are being coated with electroless nickel and after coating, the mandrels will be diamond turned. The prescription is cut into the mandrel during this diamond turning step. After metrology is performed and the figure is verified, the mandrels will enter into the polishing phase where they will be polished until they meet the 0.5 nm surface roughness requirement. To enhance reflectivity, the telescope mirror will be coated with Iridium. Iridium is also the baseline for the spectrometer mirror pair. However, B_4C (Boron Carbide) is being considered as the coating for the spectrometer mirror pair to improve reflectivity at steeper graze angles across this spectral band.

The grating is placed after the second spectrometer mirror (SM2) in a converging cone of rays. The grating, optimized for this configuration, has a highly chirped varied line space ruling, with ruling frequencies from 2146 - 2709 lines/mm. MIT and Izentis LLC are producing the grating using direct e-beam lithography on a planar silicon substrate, about 10 mm thick. The silicon substrate will be selected so the {111} crystal face matches the 1.5° blaze angle.

Over the past few years, MSFC has developed high-performance science cameras suitable for sub-orbital sounding rocket instruments. This suite of science cameras has demonstrated stable, low noise (less than 5 e^- read noise) performance.[8,9] The MaGIXS detector is an e2v 2k × 2k frame transfer CCD, with 15 × 15 μm pixels. The CCD has a 2k × 1k active detection region and 2k × 1k masked region that is utilized for storing charge during frame transfer. The camera boards and chassis will be identical to the Hi-C 2 camera, which will fly this summer on 19 July. The Hi-C 2 camera has heritage from the Chromospheric Lyman-alpha Spectropolarimeter (CLASP)[10] mission that successfully launched in September 2015 and obtained unprecedented observations of Lyman-alpha polarization in the chromosphere.

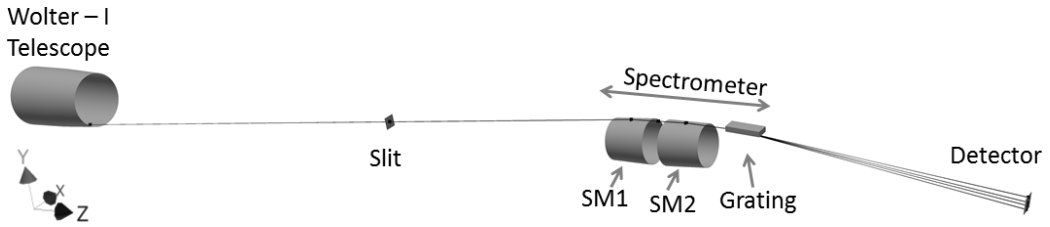

Figure 1: MaGIXS optical layout.

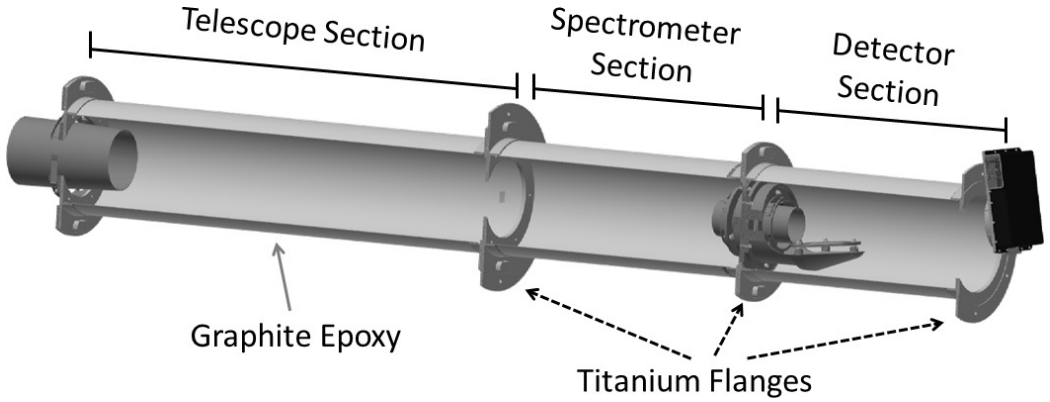

Figure 2: Layout of the MaGIXS payload. The opto-mechanical structure consists of a graphite epoxy tube with titanium interface flanges bonded to the ends. The payload is composed of 3 sections and at the interface of each section shims will be added to adjust for focus of the telescope and spectrometer independently. The mirror mounts will also interface to the titanium flanges and alignment will be maintained using semi-kinematic mounting concepts.

2. ALIGNMENT SENSITIVITY ANALYSIS

A major contributor to system level performance is the precision to which the system is aligned. Here we describe an approach for determining sensitivity to alignment error, and subsequently the maximum allowable error for each component and sub-assembly. This process was completed using the MaGIXS *Zemax* raytrace model.

2.1 Performance Metrics

Alignment error can be modeled in *Zemax* by shifting one component, or sub-assembly, then evaluating the impact on system performance. Here, performance is defined by three parameters calculated from the model: RMS spot radius, spectral error (shift in ray coordinates at the detector plane), and vignetting. RMS spot radii were obtained from *Zemax*'s spot diagram computations and are a function of wavelength and field angle. The defined requirement for spatial resolution is given in terms of FWHM, so we assumed a Gaussian spot and approximated the FWHM from the *Zemax* spot size calculations in order to compare directly to the requirement. FWHM was approximated from RMS spot sizes as:

$$FWHM = 2\sqrt{2\ln 2}\ R_s \tag{1}$$

where R_s is the RMS spot size after some alignment error is imposed on the system. In order to maintain the spatial resolution requirement, the FWHM must be less than 15 μm, the width of a pixel.

Shift in spectral lines across the detector is obtained by taking the difference in image coordinates in the direction of dispersion, along Y axis (coordinate definitions in Figure 1). Image coordinates are also computed in the spot diagram window, under the "text" tab. The change in image coordinates is converted to shift in wavelength ($\Delta\lambda$) by multiplying by step sizes given in mm/Å. Step sizes are calculated for discrete wavelengths across the spectrum for the nominal system by taking the ratio of the difference in image coordinate over the difference in wavelength: (Y_λ - Y_{λ_0})/(λ - λ_0). The requirement for spectral resolution is 22 mÅ, so $\Delta\lambda$ must be no worse than this.

Lastly, vignetting is characterized as the percentage of rays reflected by the telescope that propagate through the downstream optics and reach the detector. Each time alignment error is imposed on the system, the percentage of rays reaching the detector is compared to the nominal 4.86%. This value is the percentage of rays that reach the detector for a perfectly aligned system, with a 50 mm diameter source centered on a 34° sector of the Wolter-I telescope. An acceptable percentage of rays (V) lost due to alignment error is $< 3\%$.

$$V = \left[1 - \frac{v_s}{0.0486}\right] \times 100 \tag{2}$$

2.2 Results and Discussion

Alignment error is caused by one or more optics shifted from its nominal position. In this case, a shift can be positional translation in X, Y, Z (coordinates defined in Figure 1), or can be related to pitch and yaw: tilt about X and Y, respectively. Stepping through the system, each optic was shifted from its nominal position in one direction at a time. For example, the first spectrometer mirror was translated along the +X axis 1 mm and the spot diagram and percentage of unvignetted rays recorded. Then the +X shift in this mirror was removed, resetting the system back to nominal before the next motion. This process was repeated for all optical elements, including the spectrometer mirror pair and spectrometer sub-assemblies, at the central (17 Å) and outer (6 Å and 24 Å) wavelengths, until the maximum error was determined, as indicated by FWHM, $\Delta\lambda$, or V.

The analysis indicated which components of the system are most sensitive to alignment error and which form of alignment error had the largest impact on performance. The main takeaway is the spectrometer mirrors (SM1 and SM2) and the grating had the largest impact on performance. SM1 and SM2 were highly sensitive to tip and tilt, in terms of system resolution. The grating was also highly sensitive to tip and tilt, and additionally to displacement along the Z axis. The Wolter-I, spectrometer mirror assembly and the spectrometer were, as expected, also sensitive to tip and tilt, but not nearly to the magnitude of the SM1, SM2 and the grating. Decentration in SM1 and SM1 had a larger impact on vignetting, causing more rays to be lost, as compared to the spatial and spectral resolution. Similarly, decentration of the grating only impacted vignetting.

The tip and tilt between SM1 and SM2 has a notably larger impact on performance as compared to the other components in the system. 5 arcseconds of tilt in either SM1, or SM2 produces a FWHM equivalent to the width of a single pixel. Interestingly, when both mirrors are tilted about their common centroid, the impact of performance is insignificant. Tilting the spectrometer mirrors as an assembly by 5 arcseconds does not change the RMS spot radius at the detector.

While the spectrometer mirrors individually have a large impact on system performance, as a subassembly they have much less of an impact. Once the mirrors are mounted, aligned to one another and the configuration locked down, sensitivity to alignment error between SM1 and SM2 diminishes. Tangibly, the spectrometer mirror assembly can be tilted up to 0.1 degrees before FWHM reaches the 15 μm threshold. Figure 3 demonstrates sensitivity to tilt in the spectrometer mirrors and Table 2 is a summary table of the sensitivity analysis.

Sensitivity of the grating to pitch (tilt about X) produced a shift in the spectrum at the detector plane. Shift in line location is wavelength dependent: it is not uniform across the spectrum. What was observed is the shift at shorter wavelengths is smaller compared to the shift at longer wavelengths on the other end of the spectrum. Despite this distortion in the spectra, the spot is not blurred . Positional error of the grating in the Z axis more than 5 microns will increase vignetting of the edges of the field. These errors in the does not impact spot size (spatial resolution) and they can be dealt with operationally during calibration and post-flight data calibration.

System performance was weakly impacted by alignment error in the Wolter-I telescope, as compared to the spectrometer. Defocus and pitch and yaw of the telescope were the main factors that affected system performance. The telescope has a depth of focus of 112 μm, which is maximum amount of defocus in the telescope. 20 arcseconds of pitch or yaw have little impact on performance at FWHM = 0.025 μm. And any positional error in X, or Y only implies a translation of the image at the focal plane of the telescope.

3. SPECTROMETER ALIGNMENT

Using the sensitivity analysis as a guide, we were able to define an alignment process capable of achieving the tight tolerances on pitch and yaw. The mirror mounting and alignment procedure rely on a theodolite, for

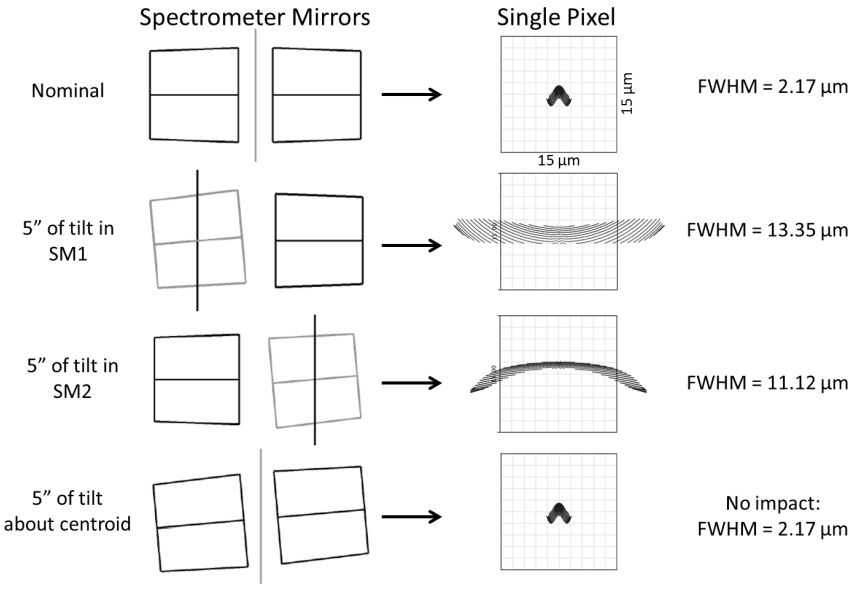

Figure 3: The spectrometer mirrors in perfect alignment produce an RMS spot radius of 0.924 μm. Tilting SM1 by roughly 5 arcseconds produces a FWHM = 13.35 μm. A similar case, SM2 tilted by 5 arcseconds produces a FWHM = 11.12 μm. Both mirrors tilted 5 arcseconds about a common centroid has zero impact on performance in the detector plane.

Element and Error Name			Unit Motion micron or arcsec or (deg)	RMS Spot Radius [μm]	FWHM [μm]	Δλ (Å)	Change in percent rays through surface (Δ%)	Vignetting Factor (%)
SM1	Decenter +X		1000	6.47	15.24	-0.02	0.01	0.21
	Decenter -X		1000	6.47	15.24	-0.02	0.01	0.21
	Decenter +Y		100	0.90	2.11	0.04	0.02	0.41
	Decenter -Y		100	0.85	0.18	0.04	0.03	-0.41
	Despace +Z		50	1.65	0.92	0.00		
	Despace -Z		50	2.31	1.06	0.00		
	About Centroid	Tilt +X asec	5	5.66	13.36	0.00	0.01	0.21
		Tilt -X asec	5	4.54	10.71	0.01	0.01	-0.21
		Tilt +Y asec	5	3.20	7.54	0.00	0.01	0.00
		Tilt -Y asec	5	3.20	7.54	0.00	0.01	0.00
SM2	Decenter +X		1000	0.93	2.20	0.00	0.07	1.44
	Decenter -X		1000	0.93	2.20	0.00	0.07	1.44
	Decenter +Y		100	0.90	2.13	0.04	0.14	2.88
	Decenter -Y		100	0.91	2.16	0.04	0.14	2.88
	Despace +Z		50	2.31	1.07	0.00		
	Despace -Z		50	1.65	0.93	0.00		
	About Centroid	Tilt +X asec	5	5.49	10.71	0.01	0.02	0.41
		Tilt -X asec	5	6.29	11.12	0.00	0.02	0.41
		Tilt +Y asec	5	3.19	5.33	0.00	0.02	0.41
		Tilt -Y asec	5	3.19	5.33	0.00	0.02	0.41
SM1 + SM2	Decenter +X		1500	4.73	11.16	0.01	0.12	2.47
	Decenter -X		1500	4.73	11.16	0.01	0.12	2.47
	Decenter +Y		30	0.94	2.22	-0.04	0.03	0.62
	Decenter -Y		30	0.91	2.15	0.04	0.03	0.62
	Despace +Z		20	1.92	0.01	0.00		
	Despace -Z		20	1.91	0.01	0.00		
	About Centroid	Tilt +X asec	20	1.88	0.11	0.00	0.08	1.65
		Tilt -X asec	20	1.80	0.26	0.00	0.01	-0.21
		Tilt +Y asec	20	1.93	0.02	0.00	0.02	0.41
		Tilt -Y asec	20	1.93	0.02	0.00	0.02	0.41
Grating	Decenter +X		2000	1.92	0.00	0.00	0.02	0.41
	Decenter -X		2000	1.92	0.00	0.00	0.02	0.41
	Decenter +Y		250	2.43	1.23	0.02	0.04	0.41
	Decenter -Y		250	1.57	0.82	0.02	0.02	0.41
	Despace +Z		5	1.93	0.03	0.01	0.02	0.41
	Despace -Z		5	1.90	0.03	0.01	0.02	0.41
	About Centroid	Tilt +X asec	5	1.92	0.01	0.02	0.02	0.41
		Tilt -X asec	5	1.91	0.01	0.02	0.02	0.41
		Tilt +Y asec	5	1.92	0.00	0.00	0.02	0.41
		Tilt -Y asec	5	1.92	0.00	0.00	0.02	0.41

Table 2: Summary of the sensitivity analysis for SM1, SM2, SM1 and SM2 pair, and the grating.

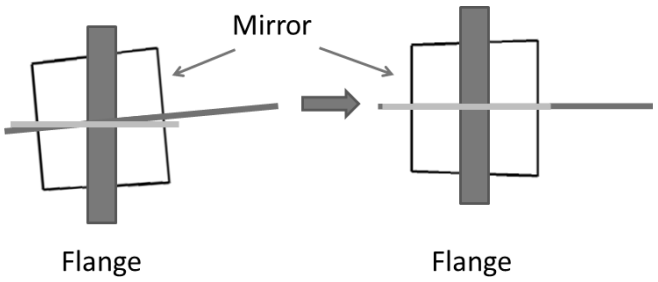

Figure 4: The goal is to align the optical axis of the grazing incidence mirror with the mechanical axis of the mounting flange. The axes must be concentric to better than 20 microns and parallel to better than 10 arcseconds.

angular alignment, and a device called the centroid detector assembly to finely align the optical axes of the components.

The centroid detector assembly (CDA), which was originally designed to align the Wolter-I nested mirror segments for AXAF,[11] will be used to monitor the positions of the mirrors. The CDA emits a beam, which can be steered to specific points on the aperture, and is able to compare the return beam to an internal reference. After the objective lens, a beam splitter picks off a reference beam and sends it directly to the CDA detector. The test beam propagates out of the CDA, through the system under test and is retro-reflected back to the CDA, where it is imaged onto the detector. A full description of the CDA is given in reference 11.

3.1 Mirror Mounting

The first alignment step aims to establish the optical axis of the mirror mounting flange and the grazing incidence mirror, and get both axes concentric to < 300 μm and parallel to < 10 arcseconds. Once this accomplished, the mirror is bonded in place to the mounting flange. This procedure is performed for the Wolter-I and both of the spectrometer mirrors. Figure 4 is a simple illustration of what is begin accomplished by this first step.

The setup makes use of a large reference flat (406 mm diameter), a 45° turning mirror (378 mm diameter), theodolite and the CDA. The reference flat is positioned horizontally on the optical bench, while the 45 degree turning mirror is positioned above it. The turning mirror is first aligned 45° from perpendicular to gravity. The theodolite will be mounted to the lab bench an adjusted to 45° of elevation. The turning mirror will be tip and tilt corrected until the return is centered in the theodolite reticle. The reference flat will be aligned perpendicular to gravity by also using the theodolite and the turning mirror. Mounted to the lab bench, perpendicular to gravity, the theodolite sends an outgoing beam aimed at the center of the turning mirror, which reflects off the reference flat, back through the turning mirror to the theodolite. The reference flat is tip and tilt corrected until the return is centered in the theodolite reticle. The setup, after alignment, is illustrated in Figure 5.

The mirror mounting flange is placed in the setup, between the fold mirror and the reference flat. A 19 mm diameter reference mirror is bonded to the flange and is used in conjunction with the theodolite to align the flange to the reference flat. The axis of the mounting flange is now parallel to the optical axis of the system, but is not yet concentric. The theodolite is replaced by the CDA and its optical axis is aligned to the established optical axis of the setup (Figure 6, left panel). An aperture plate, with a pinhole positioned in the center, is attached the mounting flange and the assembly is translated in the plane perpendicular to the optical axis until the CDA beam passes through the pinhole and is retro-reflected back to the CDA (Figure 6, right panel). Now the axis of the mirror mounting flange is parallel and concentric with the optical axis of the setup.

The aperture plate is removed from the flange and the grazing incidence is mirror placed in the center of the flange. The mirror is supported by a low-stress mount, which will hold the mirror in place until it is bonded. The aperture plate is re-mounted to the flange and sits above the entrance of the mirror. In addition to the pinhole at the center, the aperture plate has several sub-apertures circumferentially placed near the edge of the plate, where the optical surface of the grazing incidence mirror is located. In this configuration, the tip and tilt

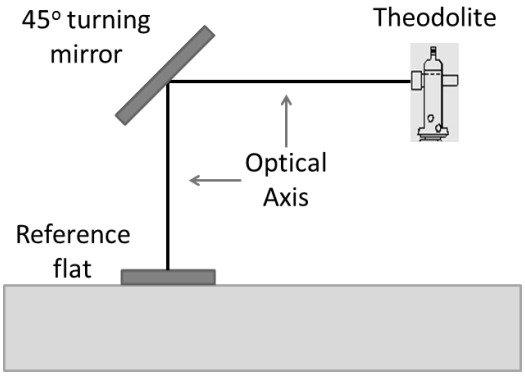

Figure 5: The fold mirror is aligned 45° from perpendicular to gravity and below it, the reference mirror is aligned perpendicular to gravity to within a few arcseconds. The black line propagating from the theodolite, through the turning mirror and the reference flat represents the optical axis of the setup. Because of the long throw required to accommodate the focal lengths of the mirrors, a fold mirror is used to reduce the size of the setup. The reference flat is 406 mm diameter and the turning mirror is 378 mm diameter. Figure is not to scale.

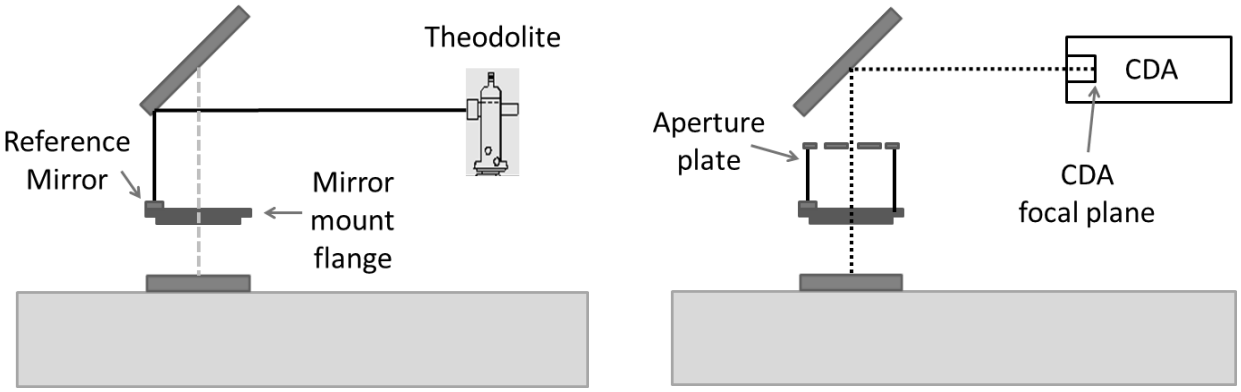

Figure 6: *Left*: The mirror mount flange is aligned using the theodolite. Tilt is removed and the axis of the flange is made parallel with the optical axis of the reference flat. *Right*: The theodolite is replaced with the CDA and an aperture plate is placed over the mounting flange. The flange is translated in the plane perpendicular to the optical axis until the CDA beam passes through the pinhole and is retro-reflected back to the CDA.

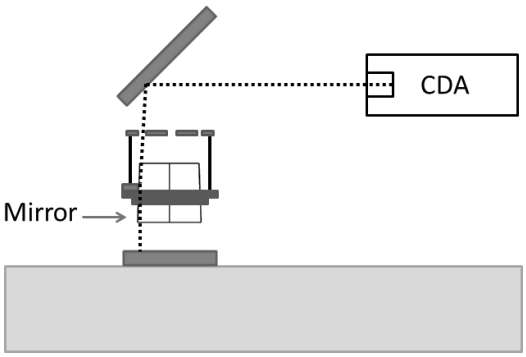

Figure 7: The mirror is placed in the setup and is supported by a mount allowing for adjustments in pitch, yaw and X, Y translation. Once the optical axis is concentric and parallel to the axis of the mounting flange, the mirror is bonded in place.

of the mirror is adjusted until the return image from each sub-aperture forms a circular ring of focused spots (Figure 7). If the mirror has tip, or tilt, the centroid of each spot corresponding to sub-apertures will not fall on a circle: the pattern will be asymmetric. When the return spot from each sub-aperture falls on a circle in the CDA detector, then the mirror axis is concentric and parallel to the mounting flange axis. The mirror is bonded in place.

3.2 Spectrometer Mirror Alignment

After the spectrometer mirrors are mounted they are integrated to the spectrometer flange and aligned to each other. The goal is to align spectrometer mirror 1 (SM1) optical axis with spectrometer mirror 2 (SM2) optical axis, then lock the configuration (Figure 8). As highlighted in the sensitivity analysis, these mirrors must be aligned to one another with no more than 5 arcseconds of error and the axes must be concentric to better than 0.1 mm.

The spectrometer flange is aligned perpendicular to gravity using the reference mirror and theodolite. This flange is the common structure to which both SM1 and SM2 are mounted to. An aperture plate is mounted to the flange, with a pinhole at the center. The CDA is placed opposite to the theodolite and the flange is translated so that the CDA beam propagates through the aperture plate. This is now the optical axis. The second spectrometer mirror, SM2, with the aperture plate attached, is placed opposite of the theodolite (refer to Figure 19). The theodolite is used to remove the tilt in the mirror flange and get the axis of the mirror parallel with the spectrometer flange axis. Getting the axes concentric is achieved by translating the mirror

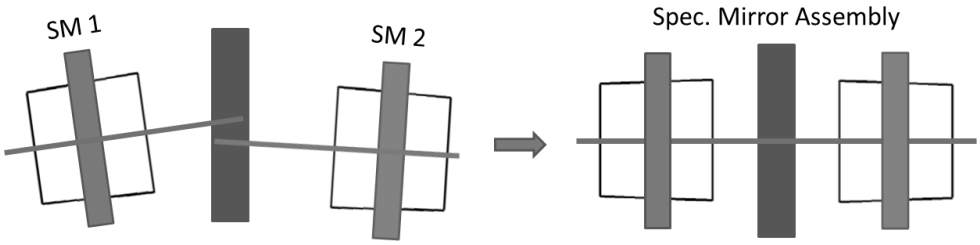

Figure 8: The goal of this step is to align the two spectrometer mirrors and mount them to a common flange. Pitch and yaw between the spectrometer mirror will be controlled by using precision machined shims and semi-kinematic ball and V-groove mounts.

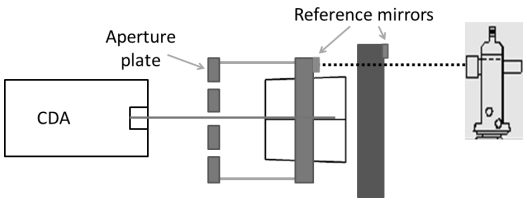

Figure 9: SM2 is aligned with the spectrometer flange using the theodolite and reference mirror. The mirror assembly is adjusted in pitch and yaw until the return to the theodolite is centered on the eyepiece reticle. The mirror assembly and spectrometer flange are both translated in the X,Y plane until the CDA beam passes through both aperture plate pinholes.

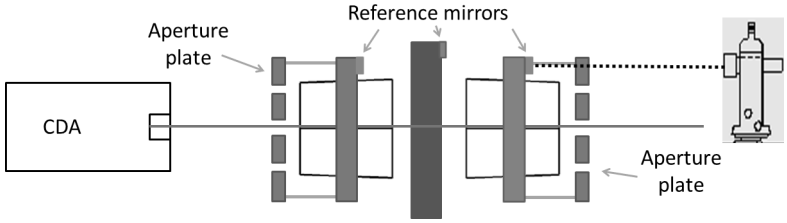

Figure 10: SM1 is integrated to the setup and is aligned to the spectrometer flange using the theodolite and reference mirror. The SM1 assembly is translated in the plane perpendicular to the optical axis until the CDA beam passes through all three aperture plates. SM1 and SM2 are now roughly aligned with each other.

flange in the plane perpendicular to the optical axis, until the beam passes through the pinhole. At this point, the spectrometer flange optical axis and SM2 optical axis are concentric and parallel.

SM1 is integrated to the setup with the aperture plate installed. Using the theodolite and the reference mirror on the mirror flange, the SM1 optical axis is made parallel to the spectrometer flange optical axis. SM1 is translated in the plane perpendicular to the optical axis until the mirror axis and CDA axis are concentric. This is achieved when the CDA beam passes through both of the aperture plates attached to SM1 and SM2, refer to Figure 10. Then SM1 is mounted to the spectrometer flange using 3 semi-kinematic spherical ball and V-groove contacts. The V-groove blocks used in the semi-kinematic mounts rest on shims, which will be machined and polished during this process to correct for tilt. We rely on these precision polished shims to achieve better than 5 arcseconds alignment error. Once the requirement is satisfied, the configuration is locked down.

The alignment of the spectrometer mirrors will be verified using the CDA. The CDA beam is steered around the sub-apertures in the aperture plate and a detector will image the focused spots. The location of the centroids of the focused spots are tracked and a circle is fitted to these points. A well aligned system will have focused spots whose centroids trace out a nearly perfect circle at the detector. Figure 11 is an illustration of how this test is performed.

By now SM1 and SM2 are aligned with one another and meet the defined requirements. The last optical element to be integrated is the grating. The grating is aligned as if it were a flat mirror, using the CDA as a controlled beam. The grating is printed onto a gold coated silicon substrate and is reflective in visible light.

The surface of the grating and the grating mount should be parallel to within 1 arcminute. This tolerance is not driven by performance of the system, but rather the shimming mechanism for adjusting pitch and yaw. The grating mount and mechanical fixture, which it attaches to, have three ball and V-groove semi-kinematic interfaces. Like the mirror mounts, shims at the mount - fixture interface will be used to adjust pitch and yaw of the grating. Maintaining parallelism to within 1 arcminute is required for accurate angular adjustments of the grating.

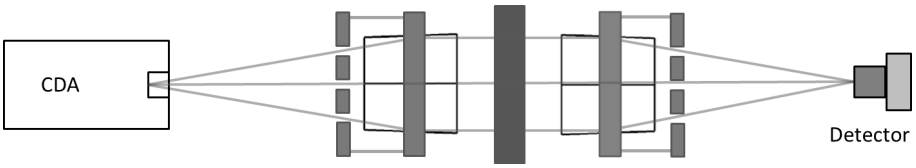

Figure 11: The CDA and a detector are both placed at the conjugate foci of the spectrometer mirrors. The tilt between the two mirrors is verified by steering the beam at several points in aperture. At each location, a the focused spot in the detector should be uniform and consistent.

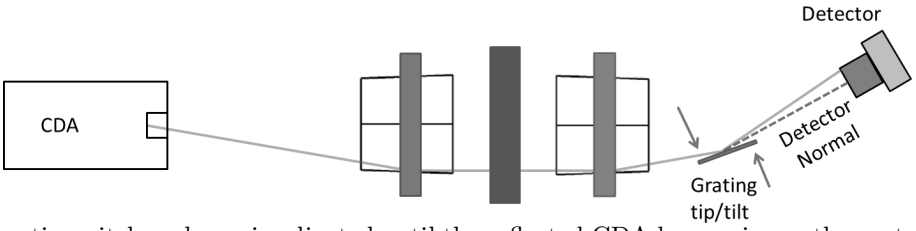

Figure 12: The grating pitch and yaw is adjusted until the reflected CDA beam pierces the center of the detector. Shims are added to offset this 0th spectral order by $\approx 3.2°$, placing the first order at the center of the detector. Fine adjustment will be performed at the detector during X-ray calibration

First the grating mount, which has a reference mirror bonded to it, is aligned perpendicular to gravity using the theodolite. The grating is integrated into the mount and is also aligned perpendicular to gravity using the theodolite, then it is bonded in place. The grating mount is integrated to the mechanical fixture, which is part of the spectrometer assembly. The detector section of the graphite epoxy opto-mechanical structure (Figure 2) is integrated with the spectrometer section and a detector is installed at the aft end of the tube. For initial alignment of the grating, the detector position does not carry tight tolerances. The detector must be positioned as accurately as ± 0.5 mm in the Z (focus) direction and $\pm$ 3 mm in the X, Y plane. The angle of the detector must be within $\pm$ 3° in pitch and yaw. During X-ray calibration, the detector will be fine tuned to the optimal position.

The CDA beam is propagated through the spectrometer mirror pair and is reflected off of the grating to the detector, as illustrated in Figure 12. The incident angle of the beam to SM1 is equal to the cone angle produced by the telescope. Pitch and yaw of the grating is adjusted until the reflected beam pierces the center of the detector. The beam is specularly reflected producing the 0th spectral order on the detector. MaGIXS operates at the 1st spectral order, so by means of the grating equation, the angular separation between these orders is well understood: 1st order is $\approx 3.2°$ from the 0th order. Using precision polished shims, the grating is adjusted so the 1st order is shifted to the center of the detector. The grating mount is locked down in this configuration and any subsequent adjustments required from the end-to-end test, or calibration will done at the detector.

Once the spectrometer is assembled and aligned, the sub-assemblies are ready to be integrate with each other and the end-to-end test performed. But first, the Wolter-I telescope is focused. The telescope section of the payload interfaces via titanium flanges to the slit flange (refer to Figure 2). For focusing of the telescope, the slit is replaced by a detector and the telescope is exposed to the X-ray beamline at the SLF. Shims are added and subtracted between the telescope section and slit flange interface, which provides a through focus scan. From this information, the best telescope focus is determined. The detector is replaced by the slit and a finite source focus spacer is placed between the telescope and the slit flange. Next, the spectrometer section and detector section (already integrated with each other) are attached to the slit flange. A second set of spacers is added and subtracted between the slit and spectrometer section for a through focus scan of the spectrometer-to-slit focus. The "best focus," the distance from the slit to the spectrometer is determined and the finite source spacer is added. With the system fully integrated, an end-to-end test is performed and alignment is verified. Fine adjustment of the detector will be performed to maneuver the spectra to the desired location on the detector.

Following the end-to-end test, the instrument is calibrated in X-rays producing effective area curves and good understanding of relative line intensities.

4. CONCLUSION

MaGIXS is the first instrument designed to observer spatially resolved, soft X-ray emission form 24 - 6.0 A (0.5 - 2.0 keV) in the solar chromosphere. The instrument, operating at grazing incidence is composed of a Wolter-I telescope and a 3-optic spectrometer. An alignment sensitivity analysis was performed to build an understanding of the required alignment and focusing accuracy that would meet optical performance and science requirements. It was found that the relative tip and tilt between the spectrometer mirror pair and tip and tilt of the grating is the most sensitive and has the largest impact of performance. A tilt in the mirrors, with respect to one another, of 5 arcseconds drives the performance out of specification (FWHM > 15 μm). With these sensitivities in mind, an approach was developed that is capable of aligning the system within these tight requirements. Verification of system alignment and X-ray calibration will be performed in the SLF at MSFC.

REFERENCES

[1] Kobayashi, K., Cirtain, J., Golub, L., Korreck, K., Cheimets, P., Hertz, E., and Caldwell, D., "Stigmatic grazing-incidence x-ray spectrograph for solar coronal observations," (2010).

[2] Kobayashi, K., Cirtain, J., Golub, L., Winebarger, A., Hertz, E., Cheimets, P., Caldwell, D., Korreck, K., Robinson, B., Reardon, P., Kester, T., Griffith, C., and Young, M., "The Marshall Grazing Incidence X-ray Spectrograph (MaGIXS)," (2011).

[3] Gubarev, M., Ramsey, B., O'Dell, S. L., Elsner, R., Kilaru, K., McCracken, J., Pavlinsky, M., Tkachenko, A., Lapshov, I., Atkins, C., and Zavlin, V., " Development of mirror modules for the ART-XC instrument aboard the Spectrum-Roentgen-Gamma mission ," (2013).

[4] Gubarev, M., Ramsey, B., Elsner, R. F., O'Dell, S., Kolodziejczak, J., McCracken, J., Zavlin, V., Swartz, D., Kilaru, K., Atkins, C., Pavlinsky, M., Tkachenko, A., and Lapshov, I., " ART-XC/SRG: status of the x-ray optics development ," (2014).

[5] Krucker, S., Christe, S., Glesener, L., McBride, S., Turin, P., Glaser, D., Saint-Hilaire, P., Delory, G., Lin, R. P., Gubarev, M., Ramsey, B., Terada, Y., Ishikawa, S.-n., Kokubun, M., Saito, S., Takahashi, T., Watanabe, S., Nakazawa, K., Tajima, H., Masuda, S., Minoshima, T., and Shomojo, M., "The Focusing Optics X-ray Solar Imager (FOXSI)," (2009).

[6] Krucker, S., Christe, S., Glesener, L., Ishikawa, S.-n., McBride, S., Glaser, D., Turin, P., Lin, R. P., Gubarev, M., Ramsey, B., Saito, S., Tanaka, Y., Takahashi, T., Watanabe, S., Tanaka, T., Tajima, H., and Masuda, S., "The Focusing Optics X-ray Solar Imager (FOXSI)."

[7] Krucker, S., Christe, S., Glesener, L., Ishikawa, S., Ramsey, B., Gubarev, M., Saito, S., Takahashi, T., Watanabe, S., Tajima, H., Tanaka, T., Turin, P., Glaser, D., Fermin, J., and Lin, R. P., " The focusing optics x-ray solar imager (FOXSI): instrument and first flight ," (2013).

[8] Champey, P., Kobayashi, K., Winebarger, A., Cirtain, J., Hyde, D., Robertson, B., Beabout, D., Beabout, B., and Stewart, M., " Performance characterization of UV science cameras developed for the Chromospheric Lyman-Alpha Spectro-Polarimeter (CLASP) ," (2014).

[9] Champey, P., Kobayashi, K., Winebarger, A., Cirtain, J., Hyde, D., Robertson, B., Beabout, B., Beabout, D., and Stewart, M., " VUV testing of science cameras at MSFC: QE measurement of the CLASP flight cameras ," (2015).

[10] Kano, R., Bando, T., Narukage, N., Ishikawa, R., Tsuneta, S., Katsukawa, Y., Kubo, M., Ishikawa, S.-n., Hara, H., Shimizu, T., Suematsu, Y., Ichimoto, K., Sakao, T., Goto, M., Kato, Y., Imada, S., Kobayashi, K., Holloway, T., Winebarger, A., Cirtain, J., De Pontieu, B., Casini, R., Trujillo Bueno, J., tpn, J., Manso Sainz, R., Belluzzi, L., Asensio Ramos, A., Auchre, F., and Carlsson, M., " Chromospheric Lyman-alpha spectro-polarimeter (CLASP) ," (2012).

[11] Glenn, P. E., "Centroid detector assembly for the AXAF-I alignment test system," (1995).